The RoboPol project: Rotations of polarization plane in optical emission of blazars

Dmitry Blinov | for the RoboPol collaboration
Univ. of Crete, Heraklion, Greece

http://robopol.org

European Union
European Social Fund
OPERATIONAL PROGRAMME
EDUCATION AND LIFELONG LEARNING
investing in knowledge society
MINISTRY OF EDUCATION & RELIGIOUS AFFAIRS, CULTURE & SPORTS
MANAGING AUTHORITY
Co-financed by Greece and the European Union
NSRF 2007-2013
EUROPEAN SOCIAL FUND

Kikuchi et al., 1988, A&A, 190, L8

PKS 1510-089

Marscher et al., 2010, ApJ 710, L126

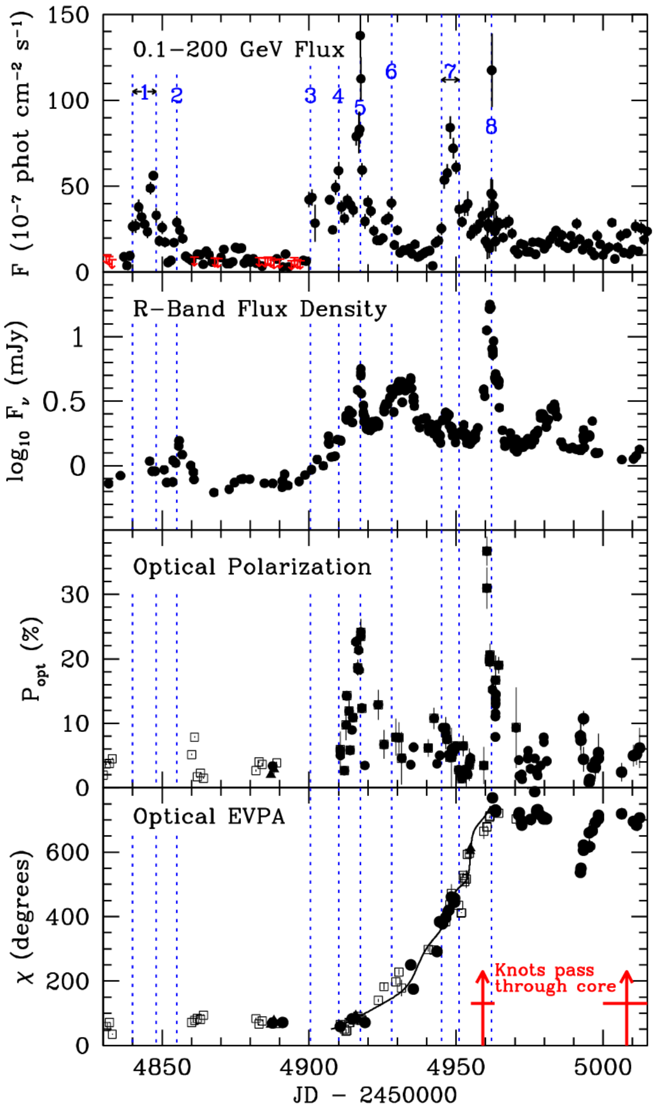

3C 279 Abdo et al., 2010, Nature 463, 919

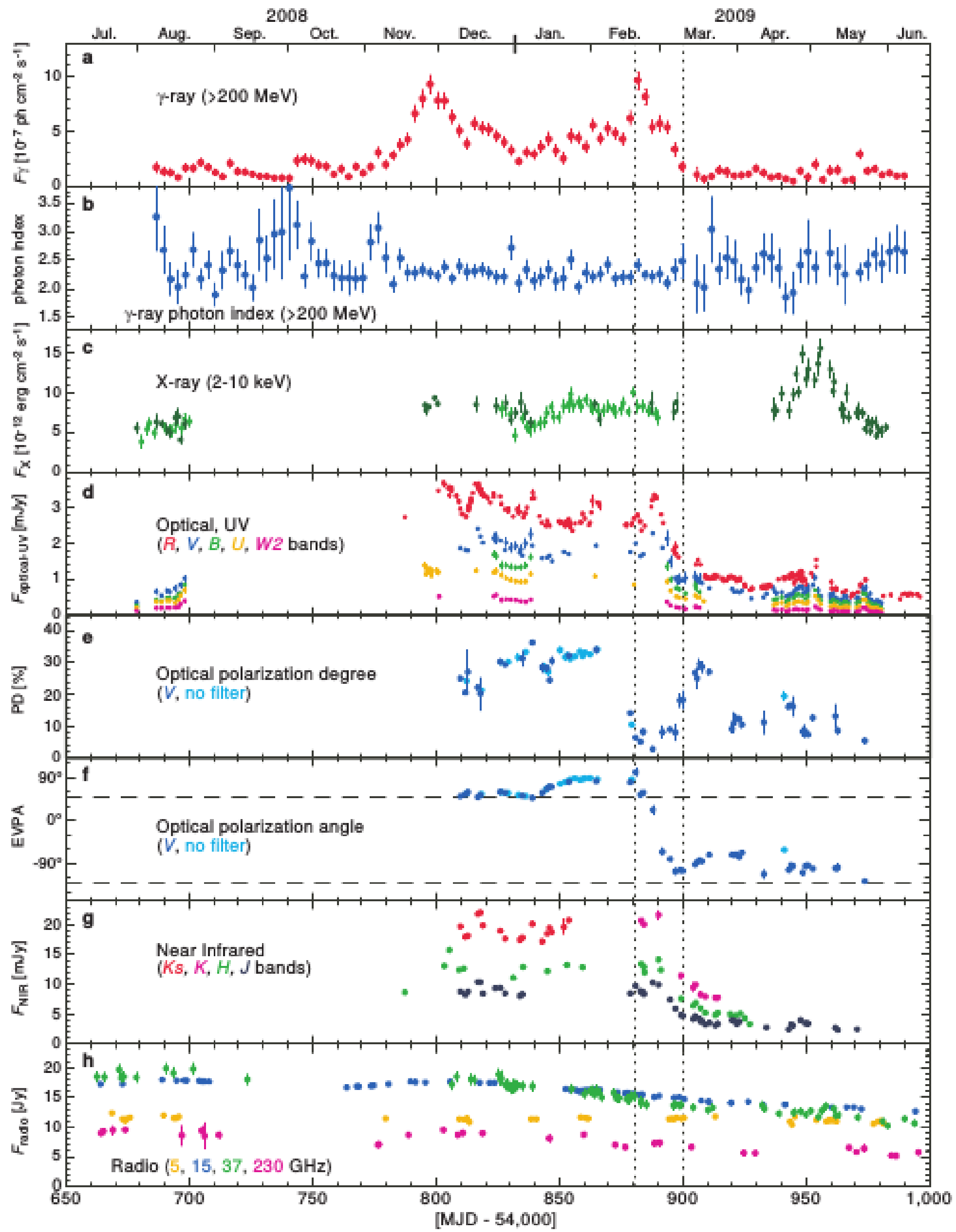

RoboPol collaboration

Caltech, USA:

M. Balokovic, T. Hovatta, O. King, T. Pearson, A. Readhead

U. of Crete/FORTH, Greece:

D. Blinov, N. Kylafis, G. Panopoulou, I. Papadakis, I. Papamastorakis, V. Pavlidou, P. Reig, K. Tassis

IUCAA, India:

P. Khodade, C. Rajarshi, A. Ramaprakash, R. Rouneq

MPIfR, Germany:

E. Angelakis, I. Myserlis, L. Fuhrmann, S. Kiehlmann, J. A. Zensus

N.C.U, Poland:

A. Kus, B. Pazderska, E. Pazderski

robopol

The project

Our approach:

- a lot of telescope time (4 nights / week) for 3 years
- built a dedicated instrument (4 channel polarimeter)
- well defined sample of blazars (84 sources)
- automated operation
- adaptive observing strategy
- broadband data (+ radio and gamma)
  OVRO, Effelsberg, Torun

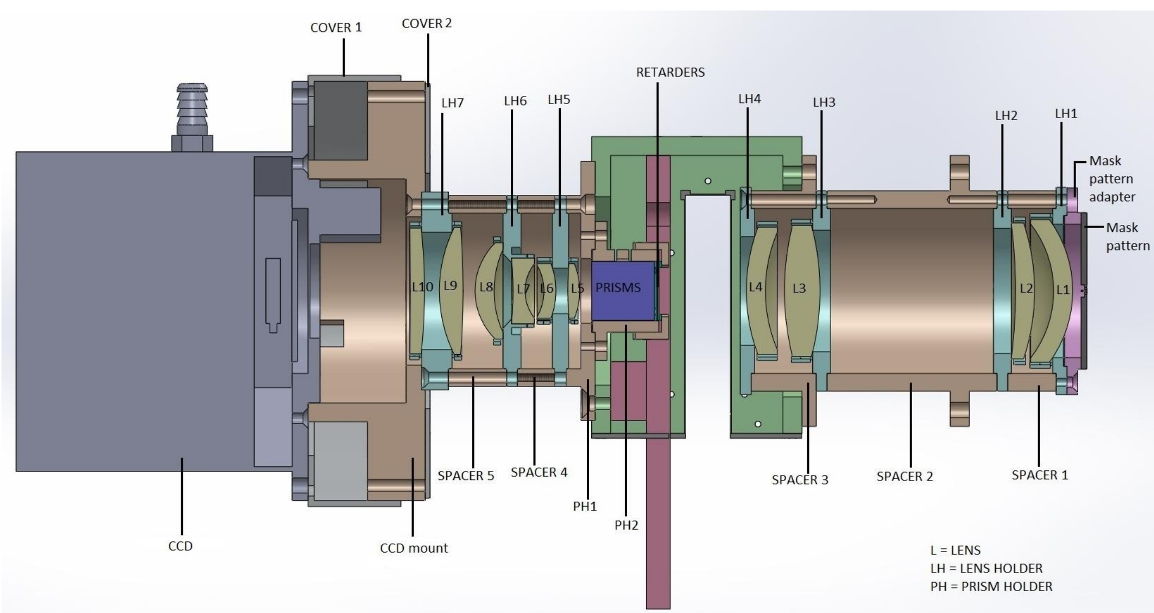

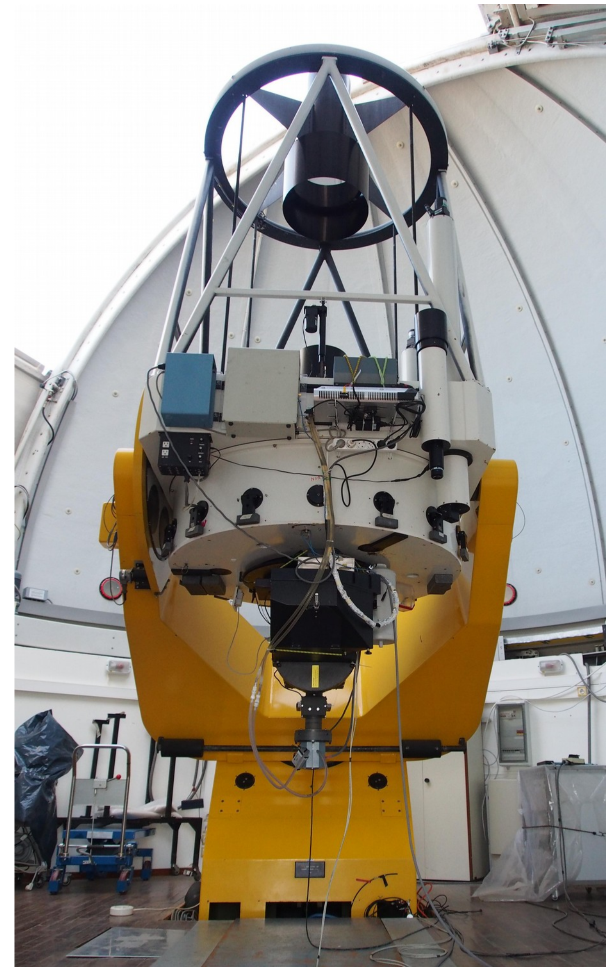

1.3 m Skinakas observatory
1750 m.a.s.l.
Median seeing 0.7'' (DIMM)

robopol

Instrument

The principal idea - no moving parts:

$$q = \frac{N_1 - N_0}{N_0 + N_1},$$

$$u = \frac{N_2 - N_3}{N_2 + N_3}$$

+ I (relative photometry)

eliminates the need for multiple exposures with different half-wave plate positions hence minimizes potential sources of error

King et al., 2014, MNRAS, 442, 1706

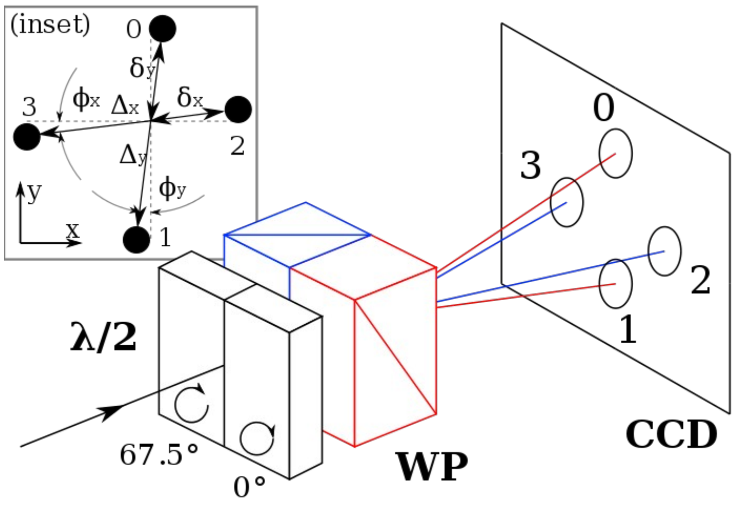

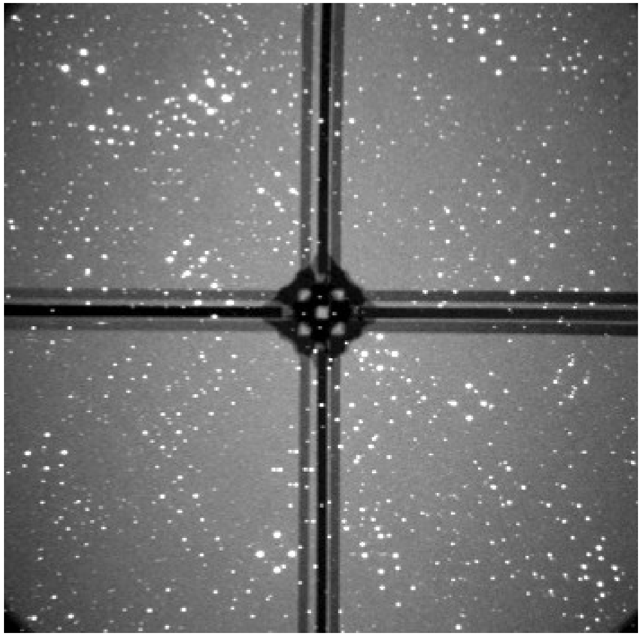

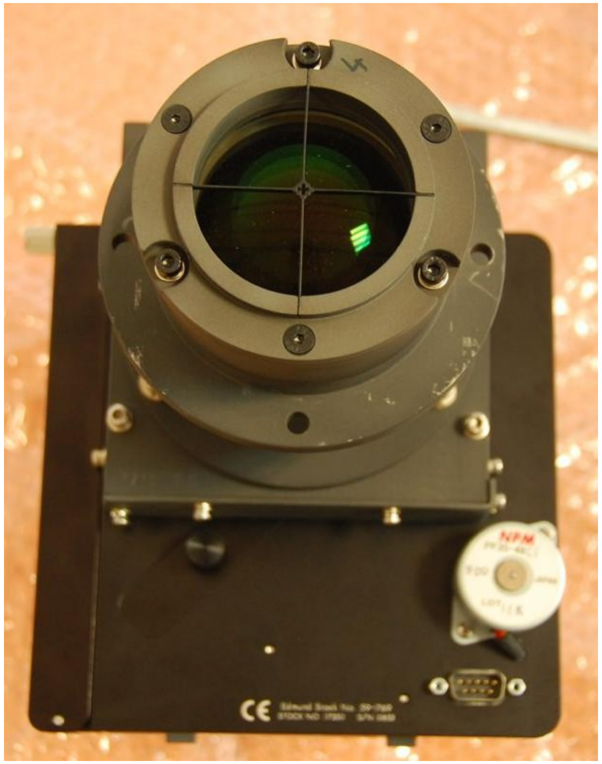

robopol

Other projects:

- magnetic fields in interstellar clouds (Tassis & Panopoulou)
- GRB afterglows (King)
- Narrow Line Seyfert 1s (Angelakis)
- TeV blazars in collaboration with Tuorla and SPbSU (Hovatta)
- X-ray binaries (Reig)
- Polarimetric standards (Ramaprakash)
- etc...

robopol

Sample

Property	Allowed range for the June survey	Allowed range for the 2013 monitoring
	Gamma-ray–loud sample	
2FGL F (> 100) MeV	$> 2 \times 10^{-8}\,\mathrm{cm}^{-2}\,\mathrm{s}^{-1}$	$> 2 \times 10^{-8}\,\mathrm{cm}^{-2}\,\mathrm{s}^{-1}$
2FGL source class	agu, bzb, or bzq	agu, bzb, or bzq
Galactic latitude $\lvert b \rvert$	$> 10°$	$> 10°$
Elevation (Elv) constraints[1]	Elv $\geqslant 30°$ for at least 30 min in June	$Elv_{max} \geqslant 40°$ for at least 120 consecutive days in the window June – November including June
R magnitude	$\leqslant 18$[2]	$\leqslant 17.5$[3]
	Control sample	
CGRaBS/15 GHz OVRO monitoring	included	included
2FGL	not included	not included
Elevation constraints[1]	None	$Elv_{max} \geqslant 40°$ constantly in the window mid-April – mid-November
R magnitude	$\leqslant 18$	$\leqslant 17.5$[2]
OVRO 15 GHz mean flux density	N/A	$\geqslant 0.060$ Jy
OVRO 15 GHz intrinsic modulation index, m	$\geqslant 0.02$	$\geqslant 0.05$
Declination	$\geqslant 54.8°$ (circumpolar)	N/A

Gamma-ray loud	142 (89 observed)	69
Control sample	25 (15 observed)	15
		+24 hand-picked sources

robopol

Survey results

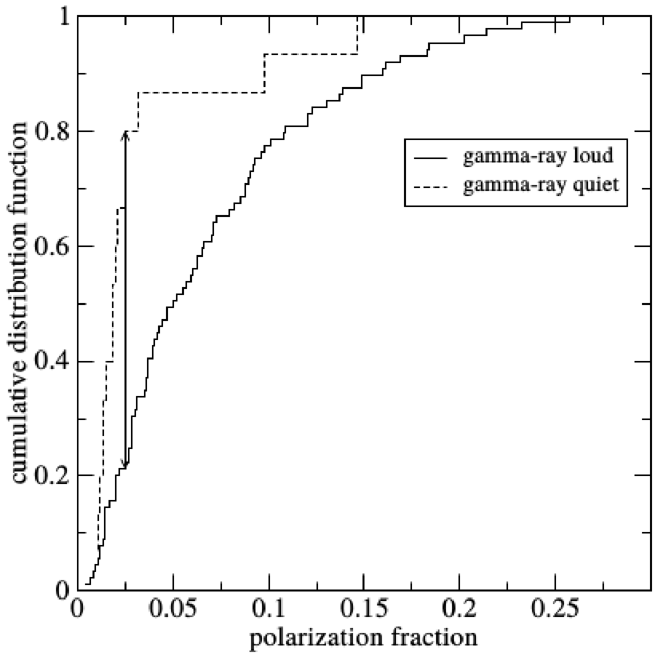

The hypothesis that polarization fractions of gamma-loud and quiet are drawn from the same distribution is rejected at 4×10^{-4} (3.5σ) level

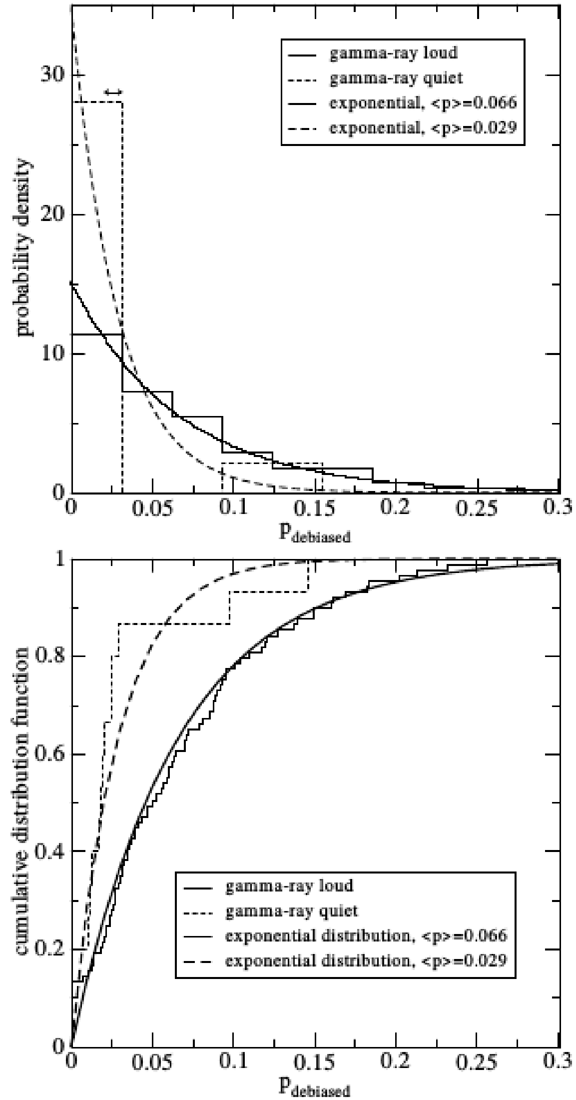

we assume:

$$P(p)dp = \frac{1}{\langle p \rangle} \exp\left(-\frac{p}{\langle p \rangle}\right) dp\,.$$

then **<p> is the parameter of the family that we want to estimate** for each population

- include only sources with $p/\sigma_p >= 3$
- to avoid biasing our results we exclude low SNR cases by:
  - split each population with R-mag = 17
  - apply low cuts at 1.5% for weak and 3.5% for bright cases
- likelihood analysis to estimate the maximum-likelihood value of the average ⟨p⟩ for each population as described by *Richards et al. (2011, ApJS, 194, 29)*

the maximum likelihood values:

- gamma-loud: 6.4 (+0.9 / -0.8) $\times10^{-2}$
- gamma-quiet: 3.2 (+2.0 / -1.1) $\times10^{-2}$

- most probable difference: 3.4 (+1.5/-2.0) $\times10^{-2}$

Pavlidou et al., 2014, MNRAS, 442, 1706

robopol

Rotations of EVPA

July – November 2013

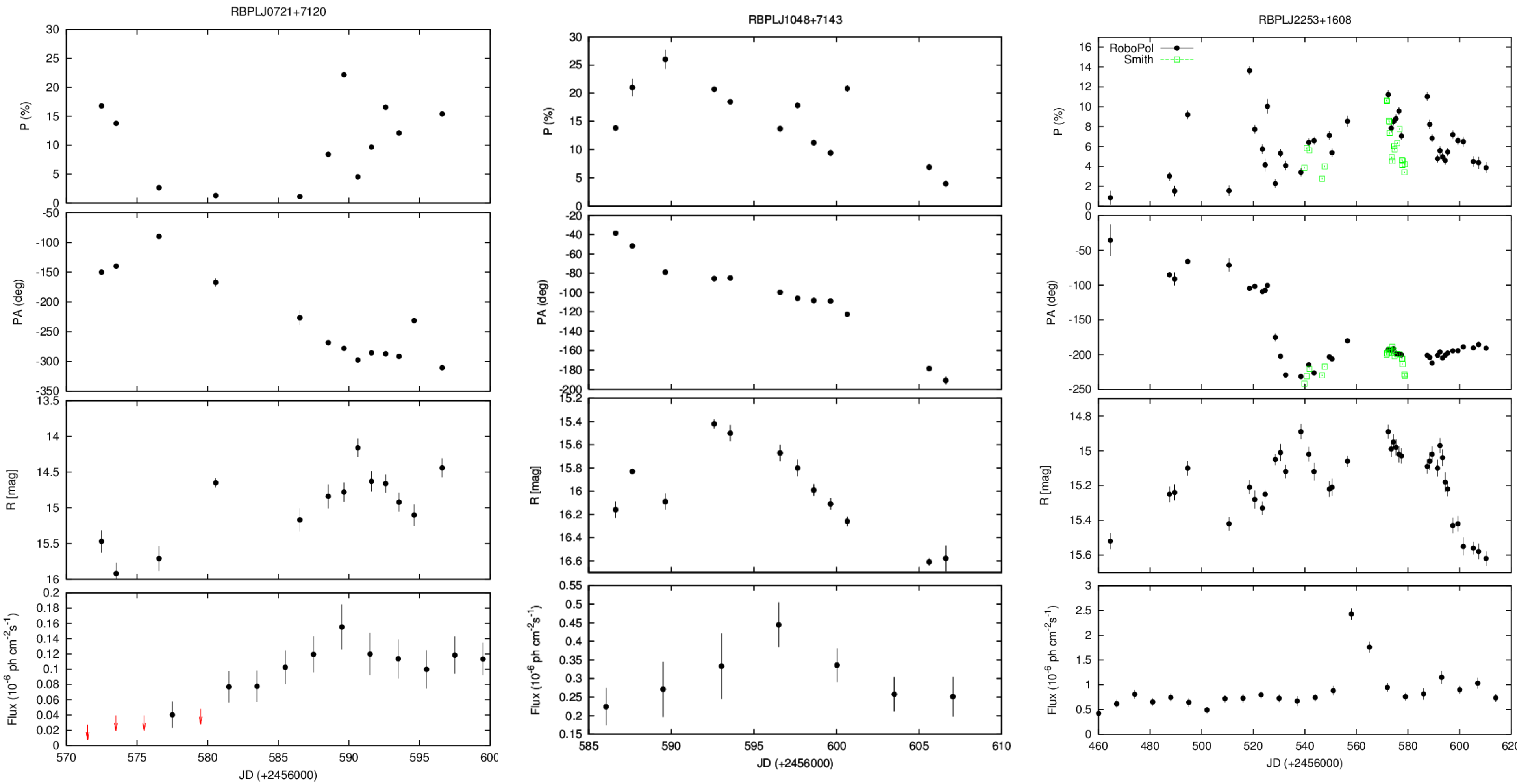

robopol

Rotations of EVPA

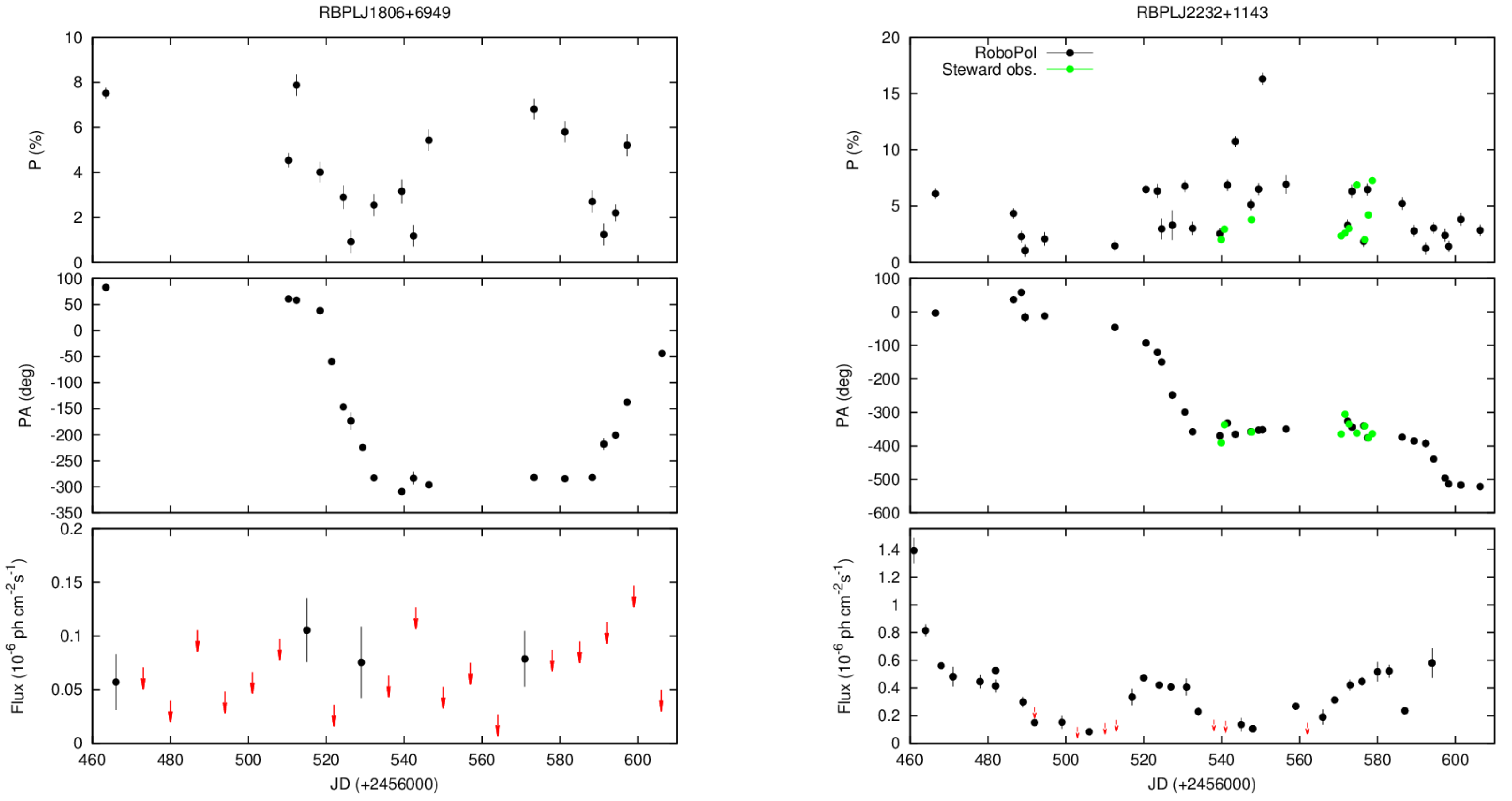

robopol

Rotations of EVPA

RoboPol id	Name	Rate[deg/day]	Length [deg]	TeV	class
RBPLJ0259+0447	PKS 0256+075	-4.5	-180	N	
RBPLJ0303+4716	TXS 0300+470	+3.3	+200	N	
RBPLJ0721+7120	S5 0716+71	-15.4	-200	Y	IBL
RBPLJ0854+2006	OJ 287	-12.7	-140	N	LBL
RBPLJ1048+7143	S5 1044+71	-7.0	-150	N	
RBPLJ1555+1111	PG 1553+113	+5.7	+130	Y	HBL
RBPLJ1558+5625	TXS 1557+565	+8.8	+220	N	
RBPLJ1806+6949	3C 371	-25.7	-360	N	
RBPLJ1927+6117	S4 1926+61	-4.8	-240	N	
RBPLJ2202+4216	BL Lac	-50.0	-250	Y	IBL
RBPLJ2232+1143	CTA 102	-20.0	-360	N	HPQ
RBPLJ2243+2021	RGB J2243+203	-5.6	-180	N	
RBPLJ2253+1608	3C 454.3	-14.0	-140	N	HPQ
RBPLJ2311+3425	B2 2308+34	+3.5	+70	N	

15 rotations in 10 blazars were known
14 new found by RoboPol
Detection rate ~1/4 (for rotations < 14deg/day)

robopol

Mechanism behind of rotations:

- stochastic variations: rotation is produced by a random walk of polarization vector on the QU plane caused by a turbulent magnetic field
Jones et al. 1985, ApJ 290, 627
Marscher 2014, ApJ 780, 87

- helical path: the rotation is caused by an emission feature moving along a helical streamline in the acceleration and collimation zone
Marscher et al. 2008, Nature 452, 966,
Marscher et al. 2010, ApJ 710, L126

- bent jet: the observed EVPA and degree change, is explained with the jet curvature, configured in such a way that the jet trajectory projected on the sky turns by ~180°
Abdo et al. 2010, Nature 463, 919

- shock passing through the jet with a helical magnetic field: several possible mechanisms
Zhang et al. 2014, arXiv: 1401.7138

robopol

Stochastic variations?

RoboPol id	Length [deg]	Occurrence [day]
RBPLJ0259+0447	-180	152
RBPLJ0303+4716	+200	203
RBPLJ0721+7120	-200	130
RBPLJ0854+2006	-140	64
RBPLJ1048+7143	-150	37
RBPLJ1555+1111	+130	132
RBPLJ1558+5625	+220	212
RBPLJ1806+6949	**-360**	**1676**
RBPLJ1927+6117	-240	351
RBPLJ2202+4216	-250	237
RBPLJ2232+1143	**-360**	**1100**
RBPLJ2243+2021	-180	174
RBPLJ2253+1608	-140	146
RBPLJ2311+3425	+70	36

Jones et al. 1985, ApJ 290, 627
Kiehlmann et al. 2013, arXiv:1311.3126
Marscher, 2014, ApJ 780, 87

MC following the algorithm described by Kiehlmann et al. 2013, arXiv:1311.3126

$$\langle P \rangle = \sqrt{\frac{\pi}{4N}} \cdot P_{\max}$$

$$\frac{N_{\mathrm{var}}}{N} = X_{\langle \Delta t \rangle} \sim \frac{\sigma(P)}{\langle P \rangle}.$$

$$X_{\Delta t} = \frac{\Delta t}{\langle \Delta t \rangle} X_{\langle \Delta t \rangle}$$

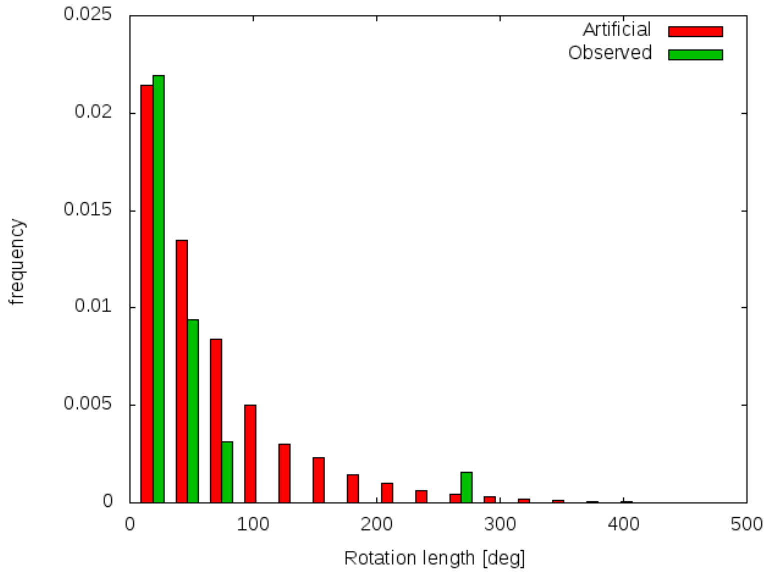

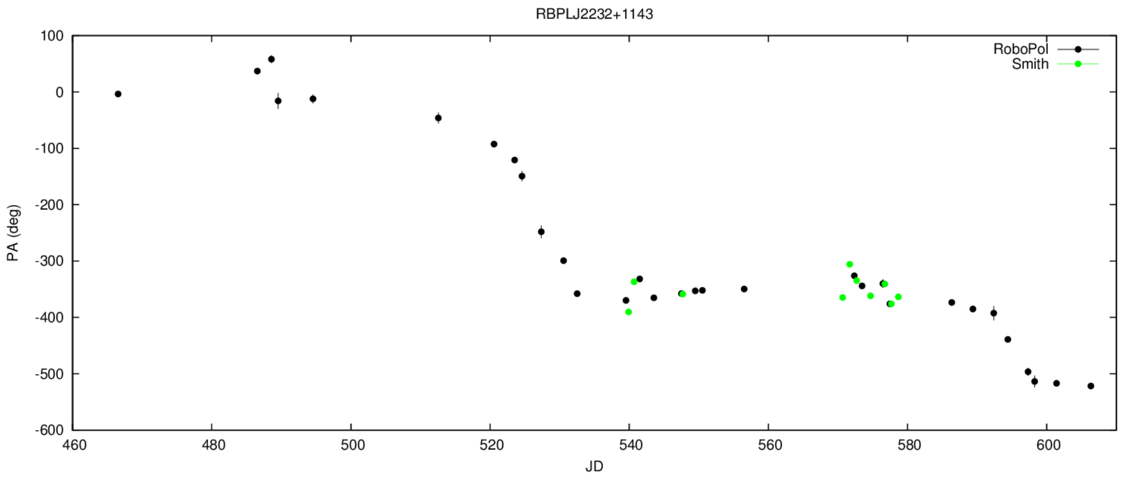

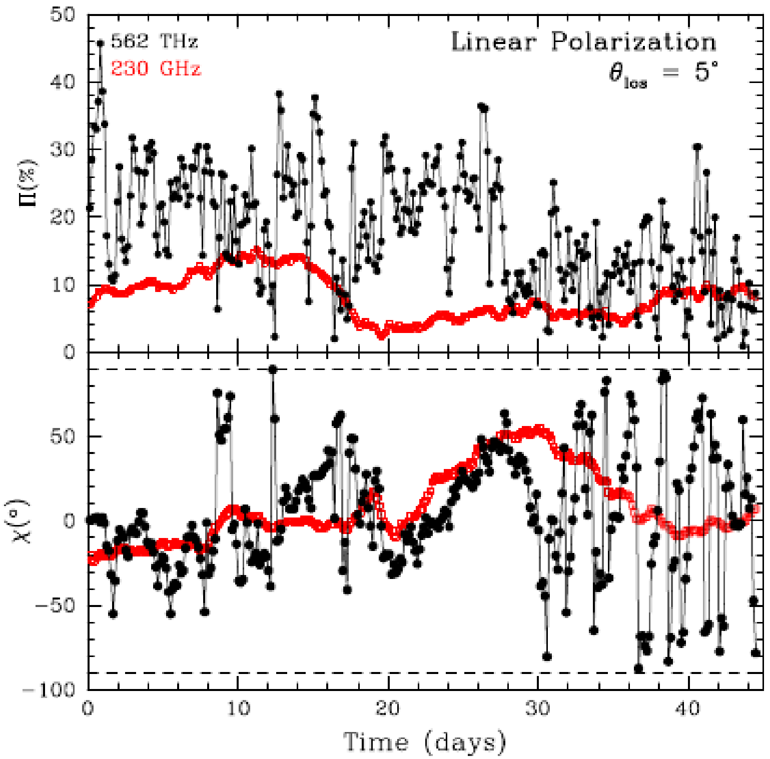

Marscher 2014, ApJ 780, 87

robopol

Connection of EVPA rotations and gamma-ray flares

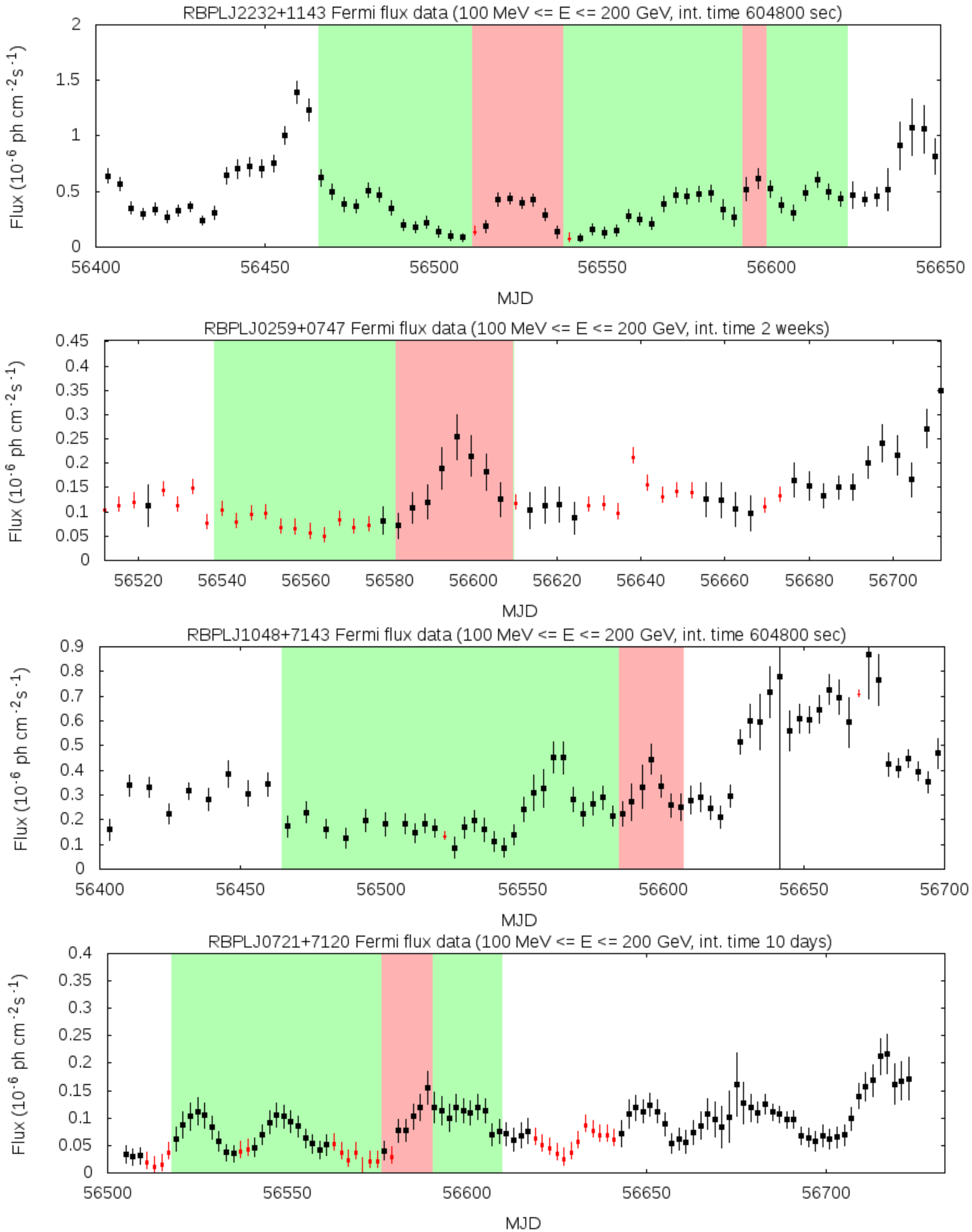

robopol

Connection of EVPA rotations and gamma-ray flares

RoboPol id	Flux (10^{-6} ph cm^{-2} s^{-1})	
	rotation	season
RBPLJ0259+0447	0.12 ± 0.02	0.08 ± 0.01
RBPLJ0303+4716	0.03 ± 0.01	0.04 ± 0.01
RBPLJ0721+7120	0.10 ± 0.02	0.07 ± 0.01
RBPLJ0854+2006	0.04 ± 0.02	0.07 ± 0.01
RBPLJ1048+7143	0.34 ± 0.03	0.23 ± 0.01
RBPLJ1555+1111	0.04 ± 0.01	0.06 ± 0.01
RBPLJ1558+5625	<0.032	0.02 ± 0.004
RBPLJ1806+6949	0.07 ± 0.02	0.05 ± 0.1
RBPLJ1927+6117	0.03 ± 0.01	0.01 ± 0.004
RBPLJ2202+4216	0.48 ± 0.10	0.31 ± 0.01
RBPLJ2232+1143	0.34 ± 0.03	0.33 ± 0.01
RBPLJ2243+2021	0.01 ± 0.01	0.01 ± 0.003
RBPLJ2253+1608	0.70 ± 0.07	0.89 ± 0.02
RBPLJ2311+3425	0.21 ± 0.03	0.21 ± 0.02

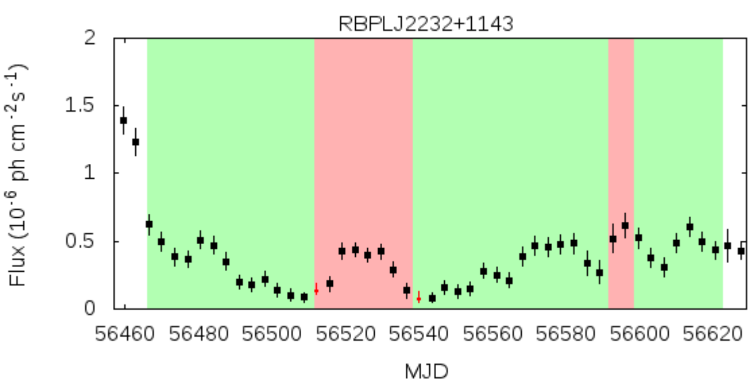

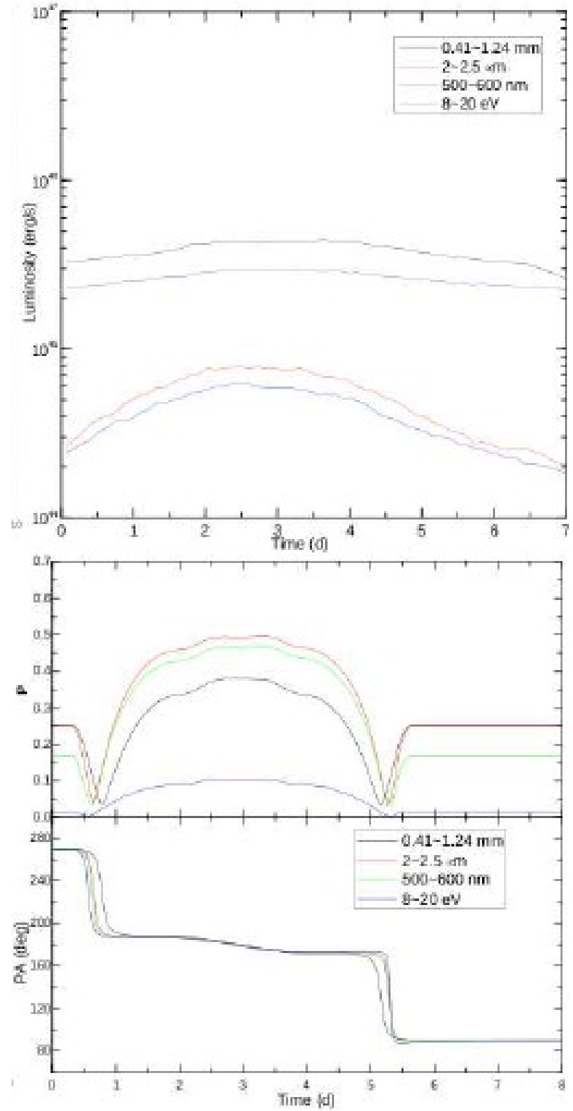

Zhang et al. 2014, arXiv: 1401.7138

robopol

Connection of EVPA rotations and gamma-ray flares

Nalewajko K., 2013, MNRAS, 430, 1324: “a flare is a contiguous period of time, associated with a given flux peak, during which the flux exceeds half of the peak value, and this lower limit is attained exactly twice – at the beginning and at the end of the flare”.

$$F(t) = F_c + \sum_{i=0}^{n} F_i \left(e^{\frac{t_i^0 - t}{T_i^r}} + e^{\frac{t - t_i^0}{T_i^d}} \right)^{-1}$$

e.g. Abdo A. A. et al., 2010, ApJ, 722, 520

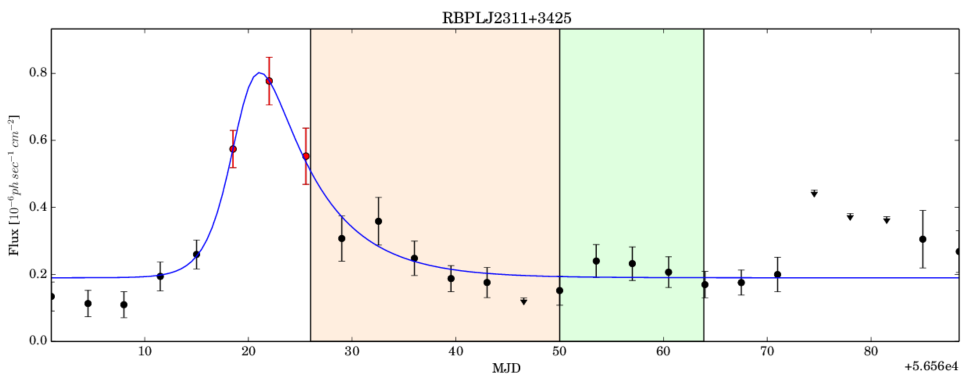

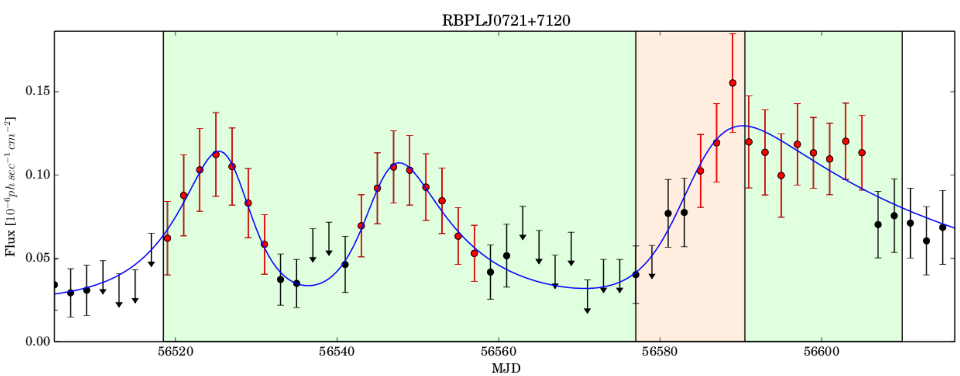

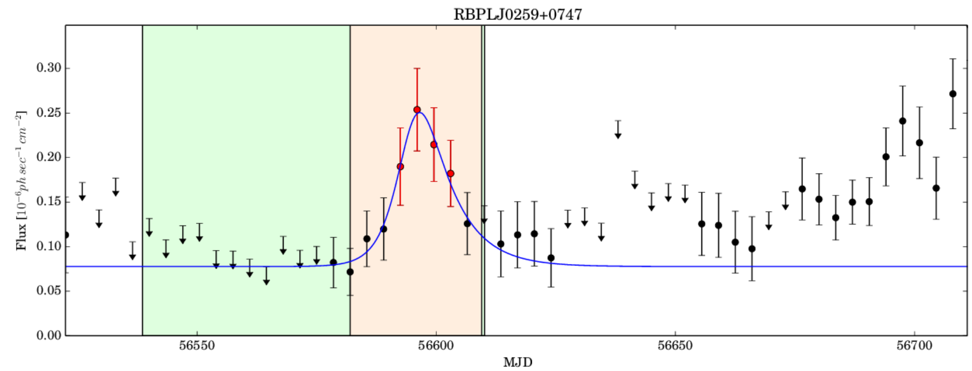

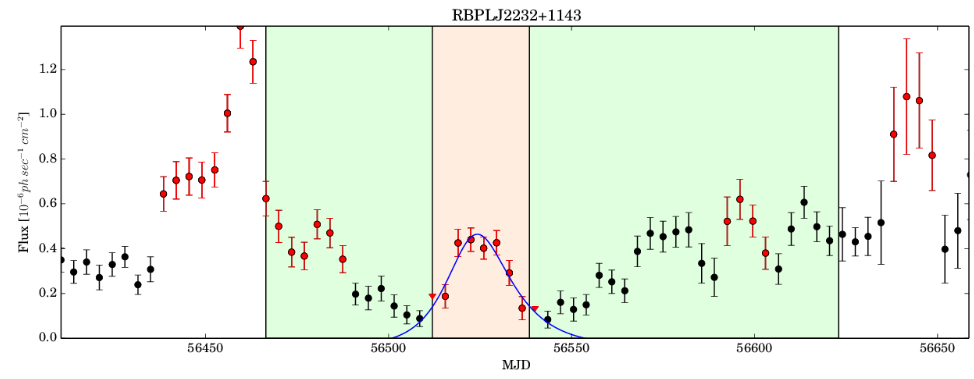

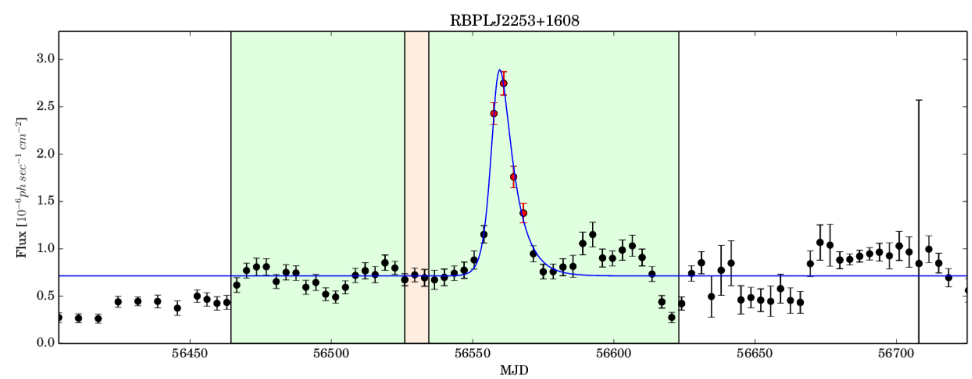

robopol

Connection of EVPA rotations and gamma-ray flares

RoboPol id	Time lag [d]	P(TL)	Rot. Occur. [day]	Rot. + Flare Occur. [day]
RBPLJ0259+0447	1.0	0.011	152	13820
RBPLJ0303+4716	-99.5	0.014	203	14500
RBPLJ0721+7120	-0.2	0.031	130	4200
RBPLJ0854+2006	-47.6	0.032	64	2000
RBPLJ1048+7143	1.2	0.032	37	1160
RBPLJ1555+1111	18.3	0.009	132	14670
RBPLJ1558+5625	-25.8	0.006	212	35300
RBPLJ1806+6949	73.8	0.012	1676	140000
RBPLJ1927+6117	8.2	0.008	351	43900
RBPLJ2202+4216	24.8	0.045	237	5270
RBPLJ2232+1143	4.0	0.033	1100	33300
RBPLJ2243+2021	27.1	0.007	174	24900
RBPLJ2253+1608	-27.8	0.015	146	9700
RBPLJ2311+3425	18.5	0.023	36	1570

Gamma properties of rotators and non-rotators

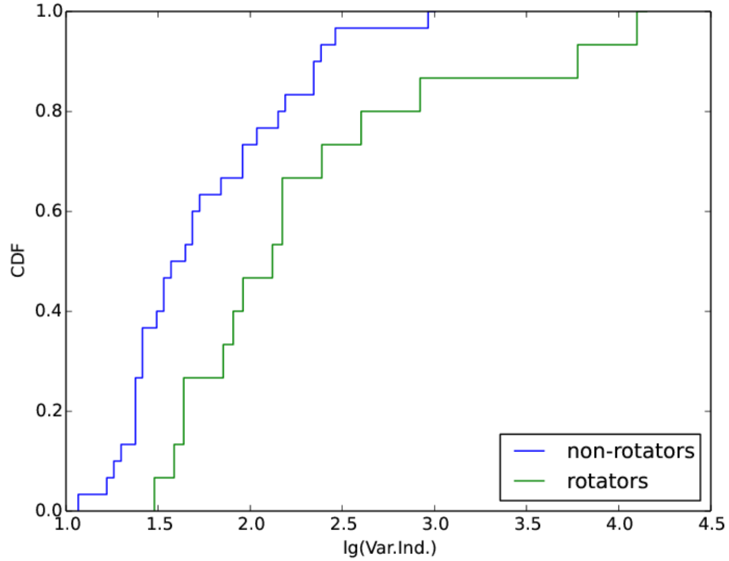

15 rotators
30 without rotations

2 sample K-S test rejects the hypothesis that samples are drawn from the same distribution at the 0.05 level

Conclusions

- Gamma-ray bright blazars have significantly higher polarization degree in optical

- All blazars with known rotations of EVPA up to date are gamma-ray bright sources

- Different blazar classes can show EVPA rotations:
high and low synchrotron peaked, FSRQs and BL Lacs, faint and bright in TeV

- Random nature of EVPA swings and their accidental coincidence with gamma-ray flares is very unfavorable

robopol